Proc. Natl. Acad. Sci. USA
Vol. 95, pp. 9654–9659, August 1998
Physiology

Human endplate acetylcholinesterase deficiency caused by mutations in the collagen-like tail subunit (ColQ) of the asymmetric enzyme

KINJI OHNO, JOAN BRENGMAN, AKIRA TSUJINO, AND ANDREW G. ENGEL*

Department of Neurology and Neuromuscular Research Laboratory, Mayo Clinic and Mayo Foundation, Rochester, MN 55905

Communicated by Clara Franzini-Armstrong, The University of Pennsylvania School of Medicine, Philadelphia, PA, May 19, 1998 (received for review April 3, 1998)

ABSTRACT **In skeletal muscle, acetylcholinesterase (AChE) exists in homomeric globular forms of type T catalytic subunits ($ACHE_T$) and heteromeric asymmetric forms composed of 1, 2, or 3 tetrameric $ACHE_T$ attached to a collagenic tail (ColQ). Asymmetric AChE is concentrated at the endplate (EP), where its collagenic tail anchors it into the basal lamina. The *$ACHE_T$* gene has been cloned in humans; *COLQ* cDNA has been cloned in *Torpedo* and rodents but not in humans. In a disabling congenital myasthenic syndrome, EP AChE deficiency (EAD), the normal asymmetric species of AChE are absent from muscle. EAD could stem from a defect that prevents binding of ColQ to $ACHE_T$ or the insertion of ColQ into the basal lamina. In six EAD patients, we found no mutations in *$ACHE_T$*. We therefore cloned human *COLQ* cDNA, determined the genomic structure and chromosomal localization of *COLQ*, and then searched for mutations in this gene. We identified six recessive truncation mutations of *COLQ* in six patients. Coexpression of each *COLQ* mutant with wild-type *$ACHE_T$* in SV40-transformed monkey kidney fibroblast (COS) cells reveals that a mutation proximal to the ColQ attachment domain for $ACHE_T$ prevents association of ColQ with $ACHE_T$; mutations distal to the attachment domain generate a mutant ≈10.5S species of AChE composed of one $ACHE_T$ tetramer and a truncated ColQ strand. The ≈10.5S species lack part of the collagen domain and the entire C-terminal domain of ColQ, or they lack only the C-terminal domain, which is required for formation of the triple collagen helix, and this likely prevents their insertion into the basal lamina.**

Acetylcholinesterase (AChE; enzyme classification 3.1.1.7) is the enzyme responsible for rapid hydrolysis of acetylcholine released at cholinergic synapses. At the normal endplate (EP), AChE limits the number of collisions between acetylcholine and the acetylcholine receptor (AChR) and, hence, the duration of the synaptic response (1). Inhibition of the enzyme results in prolonged exposure of AChR to acetylcholine, causing desensitization of AChR (2), a depolarization block at physiologic rates of stimulation (3), and an EP myopathy caused by cationic overloading of the postsynaptic region (4, 5).

Two classes of AChE are present in mammalian skeletal muscle (6, 7): (*i*) homomeric or globular forms that consist of monomers (G_1), dimers (G_2), or tetramers (G_4) of the T isoform of the catalytic subunit ($ACHE_T$), and (*ii*) heteromeric forms that consist of $ACHE_T$ subunits linked to a triple helical collagen-like tail subunit (asymmetric forms) or to hydrophobic subunits. The function of the collagen-like tail is to anchor catalytic subunits to the basal lamina. The tail is formed by the triple helical association of three collagen-like strands, ColQ. The proline-rich attachment domain (PRAD) of each strand can bind an $ACHE_T$ tetramer producing the asymmetric A_4, A_8, and A_{12} moieties (8). Asymmetric AChE is concentrated at the EP where it is the predominant species of AChE (9, 10).

In humans, all molecular forms of the catalytic subunit are encoded by one *AChE* gene (6, 11, 12). In muscle fibers, exons 2–4 (which encode the catalytic domain) spliced to exon 6 encode $ACHE_T$. *COLQ* cDNA has been cloned and sequenced from *Torpedo* electric organ (13) and rat muscle (14), and the partial genomic sequence of mouse *COLQ* has been determined (14). The sequence of the human *COLQ* gene has not been reported to date.

In 1977, Engel *et al.* (15) reported a patient with a severely disabling congenital myasthenic syndrome associated with EP AChE deficiency (EAD). Other patients with similar disorders were observed subsequently (16, 17). In these patients, AChE is absent from the EP by enzyme cytochemical and immunocytochemical criteria, and electron cytochemical studies reveal no reaction product for the enzyme in the synaptic basal lamina. Owing to absence of the enzyme from the EP, synaptic currents are prolonged and evoke repetitive muscle fiber action potentials. The presynaptic terminals are abnormally small and often are encased by Schwann cells, reducing the number of quanta released by nerve impulse, perhaps to protect the postsynaptic region from desensitization and cationic overloading. Despite reduced quantal release, at some EPs, the junctional folds degenerate, causing loss of AChR, and the junctional sarcoplasm contains apoptotic nuclei and degenerating membranous organelles. Density gradients ultracentrifugation of muscle extracts of four patients with EAD revealed no asymmetric AChE found in normal muscle, but a fifth patient who also had no AChE deposits at the EP had detectable extracted asymmetric AChE. In these patients, the kinetic properties of residual AChE in muscle as well as the activity and kinetic properties of erythrocyte AChE were normal. Mutation analysis of *$ACHE_T$* in two EAD patients not included in this report revealed no abnormality, and SV40-transformed monkey kidney fibroblast (COS) cells cotransfected with *$ACHE_T$* cloned from these two patients together with *Torpedo COLQ* readily expressed asymmetric AChE (18).

Taken together, the above findings suggest that EAD in humans who do not express asymmetric AChE stems from a defect that prevents binding of ColQ to $ACHE_T$ or the insertion of ColQ into the basal lamina. Here, we report cloning of human *COLQ* cDNA, determination of the genomic structure and chromosomal localization of the gene, and

Abbreviations: AChE, acetylcholinesterase; $ACHE_T$, T isoform of catalytic subunit; AChR, acetylcholine receptor; COS, SV-40-transformed monkey kidney fibroblast; EP, endplate; EAD, EP AChE deficiency; FISH, fluorescence *in situ* hybridization; PRAD, proline-rich attachment domain; RACE, rapid amplification of cDNA ends; RT-PCR, reverse transcription–PCR.

Data deposition: The sequence reported in this paper has been deposited in the GenBank database (accession no. AF057036).

A commentary on this article begins on p. 9070.

*To whom reprint requests should be addressed. e-mail: age@mayo.edu.

The publication costs of this article were defrayed in part by page charge payment. This article must therefore be hereby marked "*advertisement*" in accordance with 18 U.S.C. §1734 solely to indicate this fact.

identification of six truncation mutations of *COLQ* in six patients with EAD. Coexpression of each *COLQ* mutant with wild-type $ACHE_T$ in COS cells indicates that the mutant peptide either fails to assemble with $AChE_T$ or binds one tetramer of $AChE_T$ but is unlikely to insert into the basal lamina.

MATERIALS AND METHODS

Patients. Six patients with EAD, presently 12, 37, 7, 14, 8, and 2 years of age, were studied. Four were male, and two were female. Clinical and EP findings in patients 2 (15) and 3 (case 4 in Refs. 16 and 17) were reported. All had severe myasthenic symptoms since birth, negative tests for anti-AChR antibodies, a decremental electromyographic response, and failed to respond to anticholinesterase medications. Except in patient 2, supramaximal nerve stimuli evoked a repetitive compound muscle fiber action potential. Patient 6 had two siblings who died in early childhood of myasthenic symptoms; the other patients have no similarly affected relatives. Studies of intercostal muscle specimens in each patient showed absence of EP AChE, prolonged EP currents unaffected by cholinesterase inhibitors, reduced quantal release by nerve impulse, and small presynaptic endings often covered by Schwann cells. AChR channel kinetics, investigated in patients 4, 5, and 6, were normal.

Tissue Specimens. Intercostal muscle specimens were obtained from patients, and control subjects without muscle disease undergoing thoracic surgery. All human studies were in accord with the guidelines of the Institutional Review Board of the Mayo Clinic. mRNA was isolated from muscle, and DNA was isolated from muscle and blood as described (19).

Sequencing Procedures. PCR-amplified fragments were purified by the QIAquick PCR Purification Kit (Qiagen, Chatsworth, CA). Plasmids were purified by the QIAprep Spin Miniprep Kit (Qiagen) and were precipitated with ethanol. PCR products and plasmids were sequenced with an ABI 377 DNA sequencer (Perkin–Elmer) by using fluorescently labeled dideoxy terminators. PCR primers and conditions used in this study are available on request.

cDNA Cloning of Human COLQ. We used nested touchdown reverse transcription (RT)-PCR (20) to amplify and directly sequence a human *COLQ* cDNA fragment by using mouse *COLQ* primers located in PRAD and the collagen domain (14). After identifying a 76-bp fragment of human *COLQ* by homology PCR, we extended the *COLQ* sequence in the 5′ and 3′ directions by rapid amplification of cDNA ends (RACE) by using a human adult skeletal muscle cDNA library (Marathon-Ready cDNA, CLONTECH). Sequencing of the cloned RACE products revealed 3 positive 5′-RACE clones out of 11 and 4 positive 3′-RACE clones out of 14.

Analysis of Genomic Structure of COLQ. To determine the genomic structure of the human *COLQ* gene, we synthesized 38 cDNA primers and amplified and directly sequenced overlapping segments of genomic DNA by long-distance PCR. Nested inverse PCR was used to amplify untranslated regions flanking exons 1 and 1A. Control genomic DNA was digested with *Bam*HI, *Eco*RI, *Hha*I, *Hin*dIII, *Pst*I, or *Sau*3AI, was self-ligated, was amplified by inverse PCR, and was directly sequenced.

Fluorescence *in Situ* Hybridization (FISH). To determine the chromosomal localization of *COLQ*, we labeled the human *COLQ* cDNA spanning nucleotides −92 to 1,471 with digoxigenin-dUTP (Boehringer Mannheim) by the BioNick DNA Labeling System (Life Technologies, Gaithersburg, MD). Human lymphocytes were stimulated by phytohemagglutinin, were cultured, and were harvested by standard procedures. The FISH protocols were as described elsewhere (21).

Mutation Analysis. Because EAD in the newly identified patients could result from a mutation in either $ACHE_T$ or *COLQ*, we searched for mutations in both genes. We first analyzed $ACHE_T$ by amplifying and directly sequencing coding exons 2–4 and 6 and their flanking intronic regions (22). To search for mutations in *COLQ*, we used the partial genomic sequence obtained as described above and amplified and directly sequenced 17 genomic DNA fragments covering 19 constitutive and 2 alternatively transcribed exons and their flanking intronic or untranslated regions. In patients 1, 3, 4, and 5, we also directly sequenced overlapping RT-PCR products spanning the entire *COLQ* coding region. After identifying mutations in *COLQ*, we screened the patients' relatives for the observed mutations by restriction analysis or allele-specific PCR.

Construction of Expression Vectors. We amplified the entire coding regions of $ACHE_T$ (nucleotides −189 to 1,853) and *COLQ* (nucleotides −92 to 1,471) from normal muscle mRNA, cloned each product into the pTargeT Expression Vector (Promega), and confirmed the absence of PCR artifacts by sequencing the entire inserts. We introduced the S169X, E214X, R282X, 788insC, and 1082delC mutations into *COLQ* cDNA in the pTargeT vector by using the QuickChange Site-Directed Mutagenesis kit (Stratagene) as described (23). To eliminate exons 2 and 3 (107del215) from *COLQ*, we used the Seamless Cloning kit (Stratagene). The presence of desired mutations and the absence of unwanted mutations was confirmed by sequencing the entire insert, the promoter, and the polyA signal region.

Expression in COS Cells. COS-7 cells were grown and were transfected 1 day after spreading by the DEAE-dextran method (24) with 5 μg of $ACHE_T$ cDNA and 5 μg of wild-type or mutant *COLQ* cDNA or only with 5 μg of $ACHE_T$ cDNA per 10-cm dish. The cells were collected for AChE extraction 3 days after transfection.

AChE Extraction. AChE was extracted from muscle specimens pulverized under liquid nitrogen or from COS cells with a solution containing 50 mM Tris (pH 7.0) 1 M NaCl, 0.5% Triton X-100, 0.2 mM EGTA, 2 μg/ml leupeptin, and 1 μg/ml pepstatin.

Sedimentation Analysis. Sedimentation analysis was performed in a 5–20% sucrose density gradient made up in the extraction solution. Samples contained 1 mg of protein of human muscle extract or COS cell extracts equivalent to 50–100 milli-Ellman-units of AChE and marker enzymes with known sedimentation constants: alkaline phosphatase (6.1 S), catalase (11.3 S), and β-galactosidase (16 S). Fraction numbers were converted to S values by using the linear relationship between fraction numbers and the positions of the markers in the gradient. Centrifugation was in a Beckman Ti41SW rotor at 4°C for 21 hr at 38,000 rpm. AChE activity was determined in the gradient fractions by the Ellman method (25) in the presence of 5×10^{-5} M ethopropazine, an inhibitor of butyrylcholinesterase (enzyme classification 3.1.1.8).

RESULTS

Density Gradient Studies of Muscle Extracts. Density gradient centrifugation was performed on muscle extracts of patients 1, 4, 5, and 6 and on controls. Density gradient studies in patients 2 (15) and 3 (16) were reported previously. AChE extracted from control muscles is resolved into G_1, G_2, A_4/G_4, A_8, and A_{12} components (26) (Fig. 1*A*), but the amplitudes of the A_{12} and of the G_1 and G_2 peaks vary from specimen to specimen. AChE extracted from EAD muscles has a different sedimentation profile (Fig. 1 *B–E*); the heteromeric A_{12} and A_8 species are absent and the low amplitude A_4/G_4 peak that comprises ≈9.5 and 11S components is replaced by a single mutant peak between 10 and 11 S. As in control muscles, the relative amplitudes of the G_1 and G_2 peaks vary. Similar sedimentation profiles were observed previously in patients 2 (15) and 3 (16), although the mutant peak in these patients was

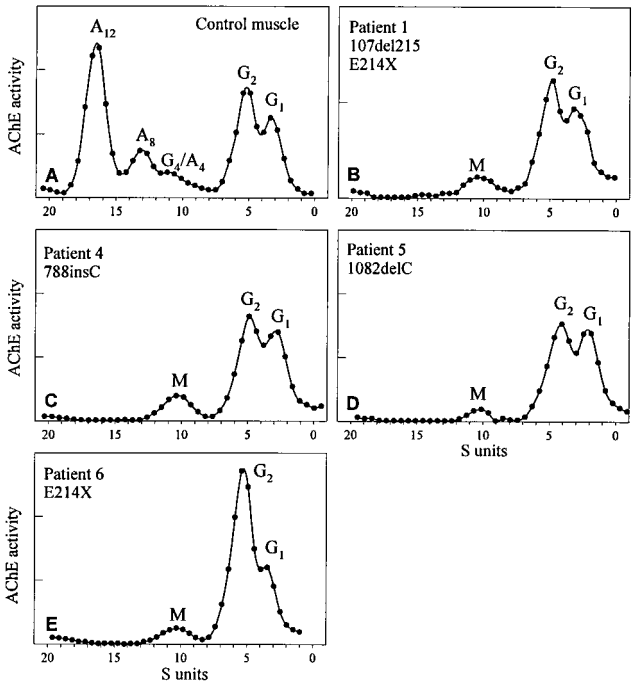

FIG. 1. Density gradient centrifugation of AChE extracted from muscle in control subject (*A*) and EAD patients 1, 4, 5, and 6 (*B–E*). Mutations in each case are indicated. *A* and *G* denote asymmetric and globular species. In each patient extract, the heteromeric A_{12} and A_8 species are absent and the composite G_4/A_4 peak is replaced by a single mutant ≈10.5S peak. (M, mutant peak.)

indistinct. Thus, patients 1–6 are deficient in the heteromeric forms of AChE. To investigate the genetic basis of this finding, we first excluded the possibility of a mutation in $ACHE_T$ that might prevent the association of the globular catalytic subunits with the collagenic tail. Direct sequencing of the entire coding region of $ACHE_T$ in each patient revealed no mutations. Next, we cloned wild-type human *COLQ* cDNA, determined the genomic structure and chromosomal localization of *COLQ*, and then searched for mutations in *COLQ*.

Cloning of Human *COLQ* cDNA. We first identified a 76-bp human *COLQ* cDNA fragment, which later proved to be nucleotides 201 to 276, by nested touchdown RT-PCR using mouse cDNA primers. Next, we extended this sequence by 5′- and 3′-RACE. By 5′-RACE, we determined nucleotides −126 to 219 and also an alternative transcriptional start site (discussed below). 3′-RACE identified nucleotides 251 to 1,504. Using the identified human *COLQ* sequence and the expressed sequence tags database, we found that sequence yw55a10.r1 of IMAGE Consortium Clone 256122 is highly homologous to the 3′ end of human *COLQ*. Sequencing the entire insert of this clone revealed that it harbored 1,149 bp of the 3′-end of the human *COLQ*, corresponding to nucleotides 1,306 to 2,454.

The above findings enabled us to identify the nucleotide sequence of the human *COLQ* from nucleotides −126 to 2,454 and the coding region as extending from nucleotides 1–1,368 (Fig. 2). We excluded PCR or cloning artifacts by directly sequencing overlapping fragments of the entire *COLQ* cDNA in two normal controls. The predicted human ColQ peptide comprises 455 amino acids. It is 89% homologous to but 3 residues shorter than the predicted rat ColQ peptide (14) and is 58% homologous to but 16 residues shorter than the predicted *Torpedo* ColQ peptide (13) (Fig. 3). Like rodent (14) and *Torpedo* (13) ColQ, human ColQ has conserved domains (Fig. 3): (*i*) a secretion signal peptide at codons 1 to 22; (*ii*) PRAD at residues 51 to 67 that interacts with $ACHE_T$; (*iii*) two adjacent cysteines at 51 and 52 that form disulfide bonds with the $ACHE_T$; (*iv*) a collagen domain composed of GXY triplets

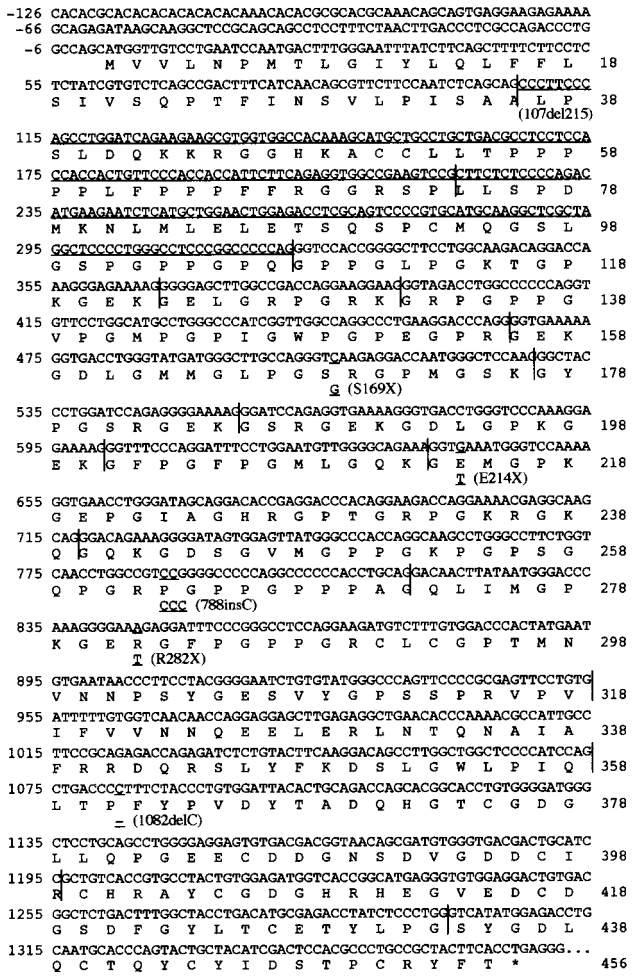

FIG. 2. cDNA sequence of the human *COLQ* gene (GenBank accession no. AF057036) and truncation mutations in the patients. Mutations are underlined. The 107del215 mutation results from skipping of exons 2 and 3. Vertical lines indicate exon boundaries. The left and right columns show nucleotide and codon numbers from the translational start site. The 3′ untranslated region is not shown.

spanning residues 96 to 291 interrupted by a noncollagenous motif at 270–276; (*v*) conserved cysteines 93, 291, and 293 that stabilize the triple helical collagen domain; (*vi*) two heparan sulfate proteoglycan binding domains at 130–133 and 235–238 implicated in anchoring the triple helical collagen domain to the basal lamina (27); and (*vii*) a C-terminal region enriched in charged residues and cysteines.

Alternative Transcripts. The 5′- and 3′-RACE and direct sequencing of RT-PCR products in normal controls disclosed seven different alternative transcripts that were not observed in other species (Fig. 4): (*i*) One starting from exon 1A substitutes 25 amino acids for 35 wild-type N-terminal amino acids. The transcript encodes a hydrophobic N terminus that may serve as a signal peptide. (*ii*) An in-frame deletion of exon 3 (nucleotides 220 to 321) that eliminates cysteine 93. (*iii*) A 13-bp deletion at nucleotides 220 to 232 caused by an activation of a cryptic splice-site in exon 3. (*iv*) An in-frame deletion of exon 5 (nucleotides 367 to 393) that abolishes a heparan sulfate proteoglycan binding domain. (*v*) A 142-bp insertion after nucleotide 717 designated exon 11A. (*vi*) A frameshifting skipping of exon 13 (nucleotides 815 to 954). (*vii*) A frameshifting skipping of exons 13 to16 (nucleotides 815 to 1,298). RT-PCR analysis detected these alternative transcripts in 32 controls with frequencies ranging from 9/32 to 28/32. The physiological significance of the alternative transcripts remains unknown.

```
Human    M                              VVLNPMTLGIYLQLFFLSIVSQPTFINSV   30
Exon 1A  -                                        TGSS-S-AHLLIISGLLCY   20
Rat      -                              A--------------C------------   30
Torpedo  -LGILLQKATATLASGLNSSRAGMF-IA--LL-----DHALAES--LDKA           50
                 107del215                 PRAD
Human    LPISAALPSLDQKKRGGHKACCLLTPPPPPLFPPPFFRGGRSPLLSPDMK   80
Exon 1A  SAGCL                                                 25
Rat      --------G-------N-------M--------------S----------   80
Mouse          --G-------S-------M--------------S----------
Torpedo  FSLQ---LPMEH--- SVNK----------M------TETN I-QEV-LN   98

Human    NLMLELETSQSPCMQGSLGSP GPPGPQGPPGLPGKTGPKGEKGELGRPG  129
Rat      -- ----A-P---------- --------------A-------D-----  128
Mouse    -- ----A-P---I------- ----------------------D-----
Torpedo  --P--IKPTEPS-KITCIIG-P--S-----Q-IQ-IM-----I--I----  148
         HSPBD                                  S169X
Human    RKGRPGPPGVPGMPGPIGWPGPEGPRGEKGDLGMMGLPGSRGPMGSKGYP  179
Rat      ------------E---V---------------V----------------F-  178
Mouse    ----------------V-------------------------------F-
Torpedo  ------VR-PR----SPCS---I--------I-LT----A-----P--LT  198
                                        E214X
Human    GSRGEKGSRGEKGDLGPKGEKGFPGFPGMLGQKGEMGPKGEPGIAGHRGP  229
Rat      ----------R-------------------------------S--------  228
Mouse    ----------R-------------------------------S-L------
Torpedo  -QK----II----QQ-I---M-VM-L--------------VS-AP-----  248
            HSPBD                                788insC
Human    TGRPGKRGKQGQKGDSGVMGPPGKPGPSGQPGR   PGPPGPPPAGQLIM  276
Rat      ----------------I---------------QGP-------S----V-  278
Mouse    ----------------I---H-----------QGP--A----S-
Torpedo  V---------T-L---   I----IM----P--P   S-L-VMSGS-H-MV  292
         R282X
Human    GPKGERGFPGPPGRCLCGPTMNVNNPSYGESVYGPSSPRVPVIFVVNNQE  326
Rat      -L----------------PA--------DPM--RG-----A--------  328
Torpedo  -------L---V---D-NLPQT-V----NKFPTLINP-Q--A----DSED  342
                                        1082delC
Human    ELERLNTQNAIAFRRDQRSLYFKDSLGWLPIQLTPFYPVDYTADQHG TC  375
Rat      ---K-------------------------------------GLHHKAAWHL-  378
Torpedo  ---K---E--L---K--K---YR-TV------IA-   IQQMRQNPTGF-  389

Human    GDGLLQP  GEECDDGNSDVGDDCIRCHRAYCGDGHRHEGVEDCDGSDFG  423
Rat      ---V---  --------P--S-G--D---------Y--R-----------  426
Torpedo  --EIV-VEN--------RI-T-S--N-KQ------YLQS-L-E---K---  439

Human    YLTCETYLPGSYGDLQCTQYCYIDSTPCRYFT                   455
Rat      --K----------E-R-----S----------                   458
Torpedo  -H--KS-------E-K--S-------G-----                   471
```

FIG. 3. Alignment of the amino acid sequences of human, rat (14), partial mouse (14), and Torpedo (13) ColQ and truncation mutations in the patients. Gaps are inserted for alignment. The amino acid sequence encoded by the alternatively transcribed exon 1A also is shown. Closed arrowheads point to the first amino acid deleted by the truncation mutations. Dashes show identical amino acids. Secretion signal peptides are italicized for all species. Collagen domains consisting of GXY triplets are underlined. A black bar indicates the PRAD. Hatched bars indicate heparan sulfate proteoglycan binding domains. Open arrowheads show essential cysteines. The right column indicates codon numbers.

Genomic Structure of the Human COLQ. Overlapping long-distance PCR and nested inverse PCR revealed that human *COLQ* comprises 17 constitutive exons and 2 alternatively transcribed exons, 1A and 11A (Fig. 4). The approximate length from exons 1A to 17 is 50 kb.

FISH. The *COLQ* FISH probe hybridizes to a single chromosomal locus at 3p25 (Fig. 5) that is not near to any known neuromuscular disease locus.

Mutation Analysis. Direct sequencing of 17 constitutive exons and 2 alternatively transcribed exons of *COLQ* genomic DNA in our EAD patients revealed five truncation mutations:

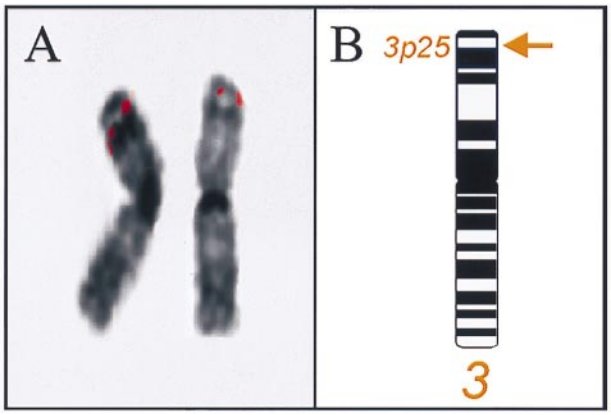

FIG. 5. Chromosomal localization of *COLQ* by FISH. *In situ* hybridization was performed by using a digoxigenin-labeled human *COLQ* cDNA probe and normal metaphase cells from stimulated blood culture. (*A*) The digitized image of the *COLQ* probe signal is localized on both chromatids of 4′,6-diamidino-2-phenylindole-enhanced G-banded chromosome 3 from reverse imaging by the Vysis SMARTCAPTURE system (Vysis, Downers Grove, IL). (*B*) *COLQ* is mapped to 3p25

E214X (patients 1 and 6), S169X (patient 2), R282X (patient 3), 788insC (patient 4), and 1082delC (patients 3 and 5) (Figs. 2–4 and 6). In addition, direct sequencing of *COLQ* cDNA in patient 1 showed another truncation mutation consisting of a large-scale frameshifting deletion (107del215) (Figs. 2–4).

Patient 1 has two heterozygous mutations, 107del215 and E214X. 107del215 is caused by the skipping of exons 2 and 3 and causes a frameshift after codon 35. This mutation abolishes PRAD and the following domains and predicts 25 missense codons followed by a stop codon. 107del215 mutation was not observed in 32 control muscle mRNA samples. Restriction analysis of the RT-PCR product reveals that the transcript harboring 107del215 has a −46G/A polymorphism. The patient and his mother are heterozygous for −46G/A (Fig. 6*A*), indicating that 107del215 is inherited from the mother. The other mutation, E214X, which truncates ColQ in the distal third of the collagen domain, is inherited from the father (Fig. 6*A*).

Patient 2 is homozygous for S169X, which results in loss of the distal two-thirds of the collagen domain. The asymptomatic mother and brother are heterozygous for S169X (Fig. 6*B*). Patient 3 is heterozygous for R282X and 1082delC. The R282X mutation truncates ColQ at 10 codons upstream to the C-terminal end of the collagen domain. 1082delC causes a frameshift after codon 360, predicting 64 missense codons followed by a stop codon. 1082delC spares the entire collagen domain but abolishes the C-terminal domain of ColQ. The asymptomatic parents are heterozygous for either of these mutations (Fig. 6*C*)

Patient 4 is homozygous for 788insC, which causes a frameshift after codon 262 predicting 36 missense codons followed by a stop codon. The 788insC mutation spares 85% of the collagen domain. The asymptomatic parents are heterozygous

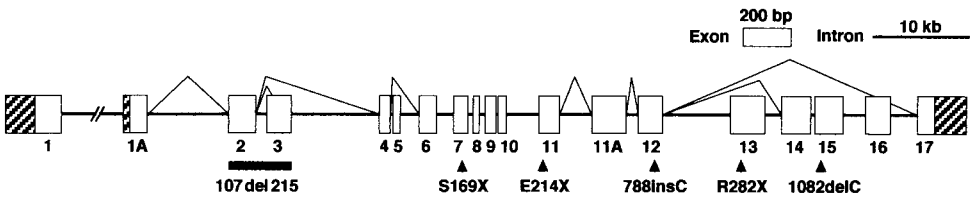

FIG. 4. Genomic structure of the human *COLQ* gene. Exons (boxes) and introns (horizontal lines) are drawn to scale. Splicing marks indicate seven alternative transcripts found in normal controls. Hatched areas show untranslated regions. Closed arrowheads indicate point mutations; black bar indicates skipping of exons 2 and 3.

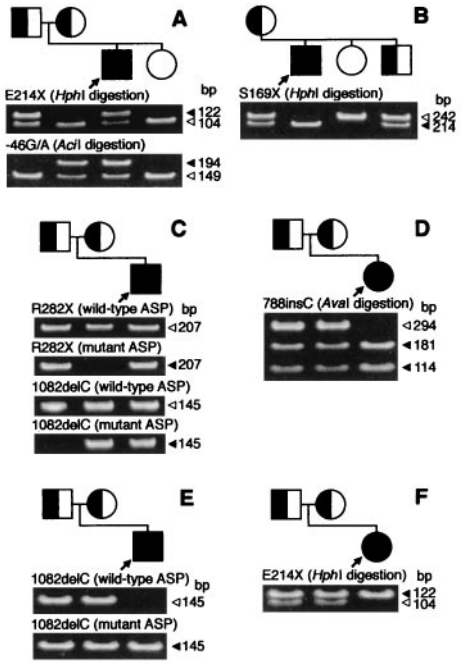

FIG. 6. Restriction analysis (*A*, *B*, *D*, and *F*) and allele-specific PCR (ASP) (*C* and *E*) using genomic DNA from patients and their respective relatives. (*A* to *F*) Families of patients 1 to 6, respectively. Closed and open arrowheads point to mutant and wild-type fragments. Closed symbols and arrows indicate patients; half-shaded symbols represent asymptomatic carriers. The −46G/A polymorphism in *A* is linked to the 107del215 mutation.

for 788insC (Fig. 6*D*). Patient 5 is homozygous for 1082delC, which is also present in patient 3. The asymptomatic parents are heterozygous for 1082delC (Fig. 6*E*). Patient 6 is homozygous for E214X. This mutation also is present in patient 1. The asymptomatic parents are heterozygous for E214X (Fig. 6*F*).

To summarize, mutation analysis reveals that patients 1 and 3 have two heterozygous mutations, and patients 2, 4, 5, and 6 have homozygous mutations. All mutations cause truncation of ColQ and are recessive, loss-of-function mutations.

Expression Studies in COS Cells. To confirm that the observed *COLQ* mutations account for the absence of asymmetric AChE in EAD, we genetically engineered each mutation into *COLQ* cDNA and coexpressed it with wild-type $ACHE_T$ cDNA in COS cells. As controls, we expressed wild-type $ACHE_T$ with or without wild-type *COLQ*.

Extracts of COS cells transfected with wild-type $ACHE_T$ and *COLQ* display the same A_{12}, A_8, and A_4 asymmetric and G_4, G_2, and G_1 globular AChE components that are detected in extracts of normal muscle (see Figs. 1*A* and 7*A*). Cells transfected only with wild-type $ACHE_T$ express prominent G_1 and G_2 peaks and a small composite peak with ≈10.5S and ≈13.5S components that likely includes nonamphiphilic G_4 molecules and an unstable nonamphiphilic higher molecular weight aggregate of the globular species (28) (Fig. 7*B*).

Cotransfection of the 107del215 mutant, which lacks PRAD, with wild-type $ACHE_T$ produces a sedimentation profile identical with that obtained after transfection with $ACHE_T$ alone (Fig. 7*C*). Thus, no moieties of asymmetric AChE are present, and the mutant peptide, if expressed, fails to bind catalytic subunits.

Cotransfection of the five other *COLQ* mutants with wild-type $ACHE_T$ produces qualitatively similar sedimentation profiles (Fig. 7 *D–H*): (*i*) None of the profiles contain the asymmetric A_4, A_8, or A_{12} moieties detected in the control extract in Fig. 7*A*. (*ii*) G_1 and G_2 peaks appear in each profile but their relative amplitudes vary. (*iii*) Each profile contains a ≈10.5S mutant peak whose sedimentation coefficient is slightly greater than that of G_4 in the control extract; this peak is prominent with S169X, E214X, 788insC, and R282X (Fig. 7

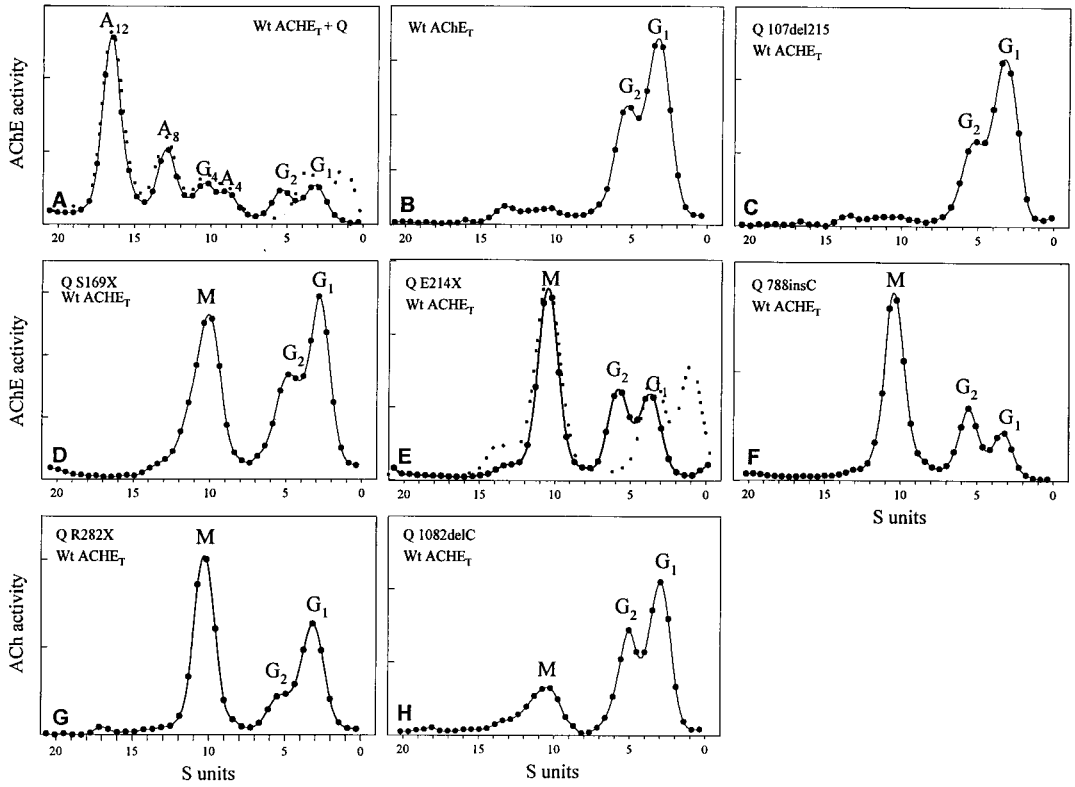

FIG. 7. Sedimentation profiles of AChE species extracted from COS cells transfected with wild-type $ACHE_T$ and *COLQ* (*A*), wild-type $ACHE_T$ (*B*), and with wild-type $ACHE_T$ plus *COLQ* mutants (*C–H*). Solid lines in all panels indicate sedimentation in the presence of 0.5% Triton X-100; interrupted lines in *A* and *E* show sedimentation in the presence of 1% Brij-97. (M, mutant peak.)

D–G) but of lower amplitude with 1082delC (Fig. 7*H*). (*iv*) A small shoulder of variable size appears left to each mutant peak (Fig. 7 *D–G*); this may correspond to an unstable nonamphiphilic higher molecular weight aggregate of the globular species (28). Centrifugation in the presence of 1% Brij-97 instead of 0.5% Triton X-100 retards the migration of the amphiphilic G_1 and G_2 peaks (28) (data shown as dotted lines for wild-type and E214X mutant in Fig. 7 *A* and *E*) but has no effect on the mutant peaks in the mutant extracts or on the asymmetric peaks in the control extract. Therefore, the mutant peaks, like the asymmetric peaks, contain nonamphiphilic catalytic subunits (6, 28). To summarize, the expression studies indicate that ColQ truncated proximal to PRAD does not associate with $ACHE_T$ and that ColQ truncated distal to PRAD results in expression of a mutant ≈10.5S species of AChE.

DISCUSSION

In this study, we first cloned the human cDNA encoding the collagen-like tail subunit of asymmetric AChE by homology PCR and RACE. We established the molecular identity of the translational product by its ability to associate with $ACHE_T$ in COS cells to yield the same asymmetric forms of AChE as detected in normal human muscle. Knowledge of the cDNA and genomic sequence of COLQ enabled us to detect truncation mutations in EAD patients. Finally, we confirmed the pathogenicity of the mutations by showing that COS cells cotransfected with wild-type *ACHE*$_T$ and each *COLQ* mutant fail to assemble the asymmetric species of AChE detected in normal muscle. The 107del215 mutation truncates ColQ N-terminal to PRAD, the domain essential for attachment of ColQ to $ACHE_T$ (8). Indeed, the mutant peptide fails to associate with $ACHE_T$ in COS cells (see Fig. 7*C*).

Four mutations distal to PRAD (S169X, E214X, 788insC, and R282X) truncate ColQ in its collagen domain, and one (1082delC) truncates it in its C-terminal domain. All of these mutations generate a nonamphiphilic ≈10.5S mutant species of AChE (see Fig. 7 *D–H*). The sedimentation coefficient of the mutant peak cannot be distinguished from that of G_4 within experimental error, but other evidence suggests that the mutant species consists of G_4 linked to the truncated peptide. First, the mutant species is not observed with 107del215 (see Fig. 7*C*); therefore, expression of the mutant depends on the presence of PRAD that can bind the catalytic subunits. Second, our expression studies are analogous to experiments by Bon *et al.* (8, 28), who cotransfected COS cells with genetically engineered truncation mutants of *Torpedo ColQ* and wild-type rat *ACHE*$_T$. *Torpedo* ColQ peptides truncated N terminal to PRAD, like our 107del215 mutant, did not bind $ACHE_T$ subunits. Peptides truncated distal to PRAD bound $ACHE_T$ tetramers to form a prominent nonamphiphilic 10.3S peak that was recognized by an anti-*Torpedo*-ColQ antibody (8, 28). Some EAD muscle extracts also contain a small mutant species (see Fig. 1), but this does not incorporate into the basal lamina. Quantitative differences between mutant species in COS cells versus EAD muscle could arise from different stabilities of the mutant transcripts or different secretion rates of the mutant proteins in the heterologous expression systems.

None of the mutant ColQs truncated distal to PRAD binds more than one $AChE_T$ tetramer to form mutant A_8 or A_{12} complexes, indicating that these mutants consist of a single peptide strand. This likely stems from the absence of the C-terminal domain that, in most collagen species, is crucial for initiating assembly of the triple helix that proceeds from a C- to N-terminal direction in a zipper-like fashion (29, 30). Triple helix formation, in turn, is essential for the clustering of basic residues of the heparan sulfate proteoglycan binding domains that serve to anchor the asymmetric forms in the basal lamina (27). Finally, the pathogenicity of the 1082delC mutant, which eliminates only the terminal 94 residues (362 to 455) of ColQ, implicates these residues as essential for triple helix formation and basal lamina insertion.

We thank Dr. S. M. Jalal, Cytogenetics Laboratory, Mayo Clinic, for assistance with FISH analysis. This work was supported by Grants NS6277 from the National Institutes of Health and by a research grant from the Muscular Dystrophy Association.

1. Katz, B. & Miledi, R. (1973) *J. Physiol. (London)* **231,** 549–574.
2. Katz, B. & Thesleff, S. (1957) *J. Physiol. (London)* **138,** 63–80.
3. Maselli, R. A. & Soliven, B. C. (1991) *Muscle Nerve* **14,** 1182–1188.
4. Salpeter, M. M., Kasprzak, H., Feng, H. & Fertuck, H. (1979) *J. Neurocytol.* **8,** 95–115.
5. Dettbarn, W. D. (1984) *Fundam. Appl. Toxicol.* **4,** S18–S26.
6. Massoulié, J., Pezzementi, L., Bon, S., Krejci, E. & Valette, F.-M. (1993) *Prog. Neurobiol.* **41,** 31–91.
7. Rotundo, R. L. & Fambrough, D. M. (1994) in *Myology,* eds. Engel, A. G. & Franzini-Armstrong, C. (McGraw–Hill, New York) 607–623.
8. Bon, S., Coussen, F. & Massoulié, J. (1997) *J. Biol. Chem.* **272,** 3016–3021.
9. Hall, Z. W. (1973) *J. Neurobiol.* **4,** 343–361.
10. Younkin, S. G., Rosenstein, C., Collins, P. L. & Rosenberry, T. L. (1982) *J. Biol. Chem.* **257,** 13630–13637.
11. Schumacher, M., Maulet, Y., Camp, S. & Taylor, P. (1988) *J. Biol. Chem.* **263,** 18979–18987.
12. Maulet, Y., Camp, S., Gibney, G., Rachinsky, T. L., Ekstrom, T. J. & Taylor, P. (1990) *Neuron* **4,** 289–301.
13. Krejci, E., Coussen, F., Duval, N., Chatel, J.-M., Legay, C., Puype, M., Vandekerckhove, J., Cartaud, J., Bon, S. & Massoulié, J. (1991) *EMBO J.* **10,** 1285–1293.
14. Krejci, E., Thomine, S., Boschetti, N., Legay, C., Sketelj, J. & Massoulié, J. (1997) *J. Biol. Chem.* **272,** 22840–22847.
15. Engel, A. G., Lambert, E. H. & Gomez, M. R. (1977) *Ann. Neurol.* **1,** 315–330.
16. Hutchinson, D. O., Walls, T. J., Nakano, S., Camp, S., Taylor, P., Harper, C. M., Groover, R. V., Peterson, H. A., Jamieson, D. G. & Engel, A. G. (1993) *Brain* **116,** 633–653.
17. Hutchinson, D. O., Engel, A. G., Walls, T. J., Nakano, S., Camp, S., Taylor, P., Harper, C. M. & Brengman, J. M. (1993) *Ann. N. Y. Acad. Sci.* **681,** 469–486.
18. Camp, S., Bon, S., Li, Y., Getman, D. K., Engel, A. G., Massoulié, J. & Taylor, P. (1995) *J. Clin. Invest.* **95,** 333–340.
19. Ohno, K., Hutchinson, D. O., Milone, M., Brengman, J. M., Bouzat, C., Sine, S. M. & Engel, A. G. (1995) *Proc. Natl. Acad. Sci. USA* **92,** 758–762.
20. Don, R. H., Cox, P. T., Wainwright, B. J., Baker, K. & Mattick, J. S. (1991) *Nucleic Acids Res.* **19,** 4008.
21. Crifasi, P. A., Michels, V. V., Driscoll, D. J., Jalal, S. M. & Dewald, G. (1995) *Mayo Clin. Proc.* **70,** 1148–1153.
22. Li, Y., Camp, S., Rachinsky, T. L., Getman, D. & Taylor, P. (1991) *J. Biol. Chem.* **266,** 23083–23090.
23. Ohno, K., Quiram, P., Milone, M., Wang, H.-L., Harper, C. M., Pruitt, J. N., Brengman, J. M., Pao, L., Fischbeck, K. H., Crawford, T. O., *et al.* (1997) *Hum. Mol. Genet.* **6,** 753–766.
24. Selden, R. F., Burke-Howie, K., Rowe, M. E., Goodman, H. M. & Moore, D. D. (1986) *Mol. Cell Biol.* **6,** 3173–3179.
25. Ellman, G. L., Courtney, K. D., Andres, V. & Featherstone, R. M. (1961) *Biochem. Pharmacol.* **7,** 88–95.
26. Bon, S., Vigny, M. & Massoulié, J. (1979) *Proc. Natl. Acad. Sci. USA* **76,** 2546–2550.
27. Deprez, P. N. & Inestrosa, N. C. (1995) *J. Biol. Chem.* **270,** 11043–11046.
28. Bon, S. & Massoulié, J. (1997) *J. Biol. Chem.* **272,** 3007–3015.
29. Dölz, R., Engel, J. & Kühn, K. (1988) *Eur. J. Biochem.* **178,** 357–366.
30. Prockop, D. J. & Kivirikko, K. I. (1995) *Annu. Rev. Biochem.* **64,** 403–434.